Regularity in chaotic reaction paths III: Ar_6 local invariances at the reaction bottleneck

Tamiki Komatsuzaki
Department of Earth and Planetary Sciences, Faculty of Science, Kobe University, Nada, Kobe 657-8501 Japan

R. Stephen Berry[a)]
Department of Chemistry and The James Franck Institute, The University of Chicago, 5735 South Ellis Avenue, Chicago, Illinois 60637

(Received 2 January 2001; accepted 21 May 2001)

We recently developed a new method to extract a many-body phase-space dividing surface, across which the transmission coefficient for the classical reaction path is unity. The example of isomerization of a 6-atom Lennard-Jones cluster showed that the action associated with the reaction coordinate is an approximate invariant of motion through the saddle regions, even at moderately high energies, at which most or all the other modes are chaotic [J. Chem. Phys. **105**, 10838 (1999); Phys. Chem. Chem. Phys. **1**, 1387 (1999)]. In the present article, we propose a new algorithm to analyze local invariances about the transition state of *N*-particle Hamiltonian systems. The approximate invariants of motion associated with a reaction coordinate in phase space densely distribute in the sea of chaotic modes in the region of the transition state. Using projections of distributions in only two principal coordinates, one can grasp and visualize the stable and unstable invariant manifolds to and from a hyperbolic point of a many-body nonlinear system, like those of the one-dimensional, integrable pendulum. This, in turn, reveals a new type of phase space bottleneck in the region of a transition state that emerges as the total energy increases, which may trap a reacting system in that region. © *2001 American Institute of Physics.*
[DOI: 10.1063/1.1385152]

I. INTRODUCTION

The questions, ''How does a system actually traverse the transition state?,'' and ''What kinds of trajectories carry the system through?,'' have been among the most intriguing subjects in chemical reaction theories over the past several decades.[1–14] Several findings, both theoretical[15–28] and experimental,[29,30] during the last decades have shed light on mechanics of passage through the reaction bottlenecks, and on the concept of transition state, especially in systems with only a few degrees of freedom (dof). The recent striking experimental studies by Lovejoy *et al.*,[29] ''see'' this transition state via the photofragment excitation spectra for unimolecular dissociation of highly vibrationally excited ketene. These spectra revealed that the rate of this reaction is controlled by the flux through quantized thresholds within a certain energy range above the barrier. The observability of the quantized thresholds in the transition state was first discussed by Chatfield *et al.*[31] Marcus[32] pointed out that this indicates that the transverse vibrational quantum numbers might indeed be approximate constants of motion, presumably in the saddle region. In the same period, Berry and his coworkers explored the nonuniformity of dynamical properties of Hamiltonian systems of several *N*-atom clusters, with *N* from 3 to 13; in particular, they explored how regular and chaotic behavior may vary locally with the topography of the potential energy surfaces (PESs).[21–28] They revealed by analyses of local Liapunov functions and Kolmogorov entropies that when systems have just enough energy to pass through the transition state, the systems' trajectories become collimated and regularized, developing approximate *local* invariants of motion different from those in the potential well. This occurs even though the dynamics in the potential well is fully chaotic under these conditions. It was also shown that at higher energies above the threshold, emerging mode–mode mixing wipes out these approximate invariants of motions even in the region of the transition state.

A widespread assumption in a common class of chemical reaction theories[1–8] is the existence of a hypersurface in phase space dividing the space into reactant and product regions, and which one might suppose a chemical species crosses only once on its path to reaction. However many formulations of chemical reaction rate theory have had to allow this probability, the ''transmission coefficient,'' to be less than unity. Davis and Gray[15] first showed that in Hamiltonian systems with two degrees of freedom (dof), the transition state defined as the separatrix in the phase space is always free from barrier recrossings, so the transmission coefficient for such systems is unity. They also showed the existence of the dynamical bottlenecks to intramolecular energy transfer, that is, cantori (in a two-dof system), which form partial barriers between irregular regions of phase space.[15–18] Zhao and Rice[17] have developed a convenient approximation for the rate expression for the intermolecular energy transfer. However, their inference depends crucially

[a)]Electronic mail: berry@uchicago.edu

on the Poincaré section having only two dimensions. No general theory exists yet for systems of higher dimensionality.[18,33–35]

Focusing on the transition state periodic orbits in the vicinity of the unstable saddle points, Pechukas, Pollak, and Child[36] first showed in the late 1970s, for two-dimensional Hamiltonian systems such as the collinear $H+H_2$ reaction, that, within a suitable energy range just above the saddle, the reaction bottleneck over which no recrossings occur with a minimal flux of the system, can be uniquely identified as one periodic orbit dividing surface (PODS), a dividing surface $S(q_1=0)$. (Here q_1 is the hyperbolic normal coordinate about the saddle point). Moreover, as the energy increases, pairs of the PODSs appearing on each reactant and product side migrate outwards, toward reactant and product state, and the outermost PODS become identified as the reaction bottleneck. De Leon and his coworkers[19] developed a so-called reactive island theory; the reactive islands are the phase space areas surrounded by the periodic orbits in the transition state region, and reactions are interpreted as occurring along cylindrical invariant manifolds through the islands. Fair, Wright, and Hutchinson[20] also found in their two-, and three-dof models of the dissociation reaction of hydrazoic acid that a similar cylinderlike structure emerges in the phase space as it leaves the transition state. However these are crucially based on the findings and the existence of (pure) periodic orbits for all the dof, at least in the region of the transition states. Hence some questions remain unresolved, e.g., ''How can one extract these periodic orbits from many-body dof phase space?'' and ''How can the periodic orbits persist at high energies above the saddle point, where chaos may wipe out any of them?''

Recently, we have developed a new method to look more deeply into these local regularities about the transition state of N-particle Hamiltonian systems.[37–41] The crux of the method is the application of Lie canonical perturbation theory (LCPT),[42–50] combined with microcanonical molecular-dynamics (MD) simulation of a region around a saddle point. This theory constructs the nonlinear transformation to a hyperbolic coordinate system, which ''rotates away'' the recrossings and nonregular behavior, especially of the motion along the reaction coordinate. We showed by using isomerization reactions in a simple cluster of 6 atoms bound by pairwise Lennard-Jones potentials that, even to high energies at which the transition state becomes manifestly chaotic, at least one action associated with the reaction coordinate remains an approximate invariant of motion over the region of the transition state. Moreover it is possible to choose a multidimensional phase-space dividing surface through which the transmission coefficient for the classical reaction path is unity;[39] We also ''visualized'' the dividing hypersurface in the phase space by constructing the projections onto subspaces of a very few coordinates and momenta, revealing how the ''shape'' of the reaction bottleneck depends on energy of the system and the passage velocity through the transition state, and how the complexity of the recrossings emerges over the saddle in the configurational space.[40,41] (The dividing hypersurface migrates, depending on the passage velocity, just as PODS do.)

Most applications of canonical perturbation theory (CPT) until now have focused on the comparisons of physical quantities, e.g., classical invariants of motion, energy levels and wave functions, calculated independently by the exact and the new Hamiltonians: the latter is transformed from the exact one as simply as possible, so that it provides classical approximate constants of motion or quasi-conserved ''good'' quantum numbers. However, the demanding problem remains to identify those parts of space (either configurational, or phase space) in which such invariants ''actually'' survive or break under the dynamics of the exact Hamiltonian, especially for many-dof systems, during the course of dynamical evolution. Beyond that is the question of how the size of a zone of approximate separability depends on the number of dof. It can be made plausible that with more dof, the more such approximate invariances develop within a locality, e.g., for certain finite durations in specific limited regions.

The purposes of the present article are these:

(1) to propose a scheme of analysis of local invariants, based on LCPT, which may be buried in the complexity of the original Hamiltonian $H(\mathbf{p},\mathbf{q})$, along the original $H(\mathbf{p},\mathbf{q})$ dynamics, without invoking an explicit assumption of its integrability at the order of LCPT one performed;
(2) to reveal, by applying this analysis to the isomerization of the Ar_6 cluster, that the invariants associated with a reaction coordinate in the phase space—whose reactive trajectories are all ''no-return'' trajectories—densely distribute in the sea of chaotic dof in the regions of (first-rank) transition states; and
(3) to show how the invariants locate in the original space $(\mathbf{p},\mathbf{q})$ and how they depend on total energy of the system and the other physical quantities, and discuss its implication for reaction dynamics, especially for many-dof systems.

The remainder of this article is organized as follows. In Sec. II, we review our method and technique. In Sec. III, we propose a concept of the duration of regularity and the procedure to calculate its location and distribution. In Sec. IV, we describe the model and the calculations. We present our results and discussion in Sec. V. Finally, we give some concluding remarks in Sec. VI. A brief account of this work has been prepared.[51]

II. THEORY

We first expand the full $3N$-dof potential energy surface about a chosen stationary point, i.e., minimum, saddle, or higher rank saddle. By taking the zeroth-order Hamiltonian H_0 as a set of harmonic oscillators, which might include some negatively curved modes, i.e., reactive modes, we establish the higher-order perturbation terms to consist of nonlinear couplings expressed in arbitrary combinations of coordinates,

$$H=H_0+\sum_{n=1}^{\infty}\epsilon^n H_n, \tag{1}$$

where

$$H_0(\mathbf{p},\mathbf{q})=\frac{1}{2}\sum_j (p_j^2+\omega_j^2 q_j^2)=\sum_{j=1} \omega_j J_j = H_0(\mathbf{J}), \tag{2}$$

$$\sum_{n=1}^{\infty} \epsilon^n H_n(\mathbf{p},\mathbf{q})$$

$$=\epsilon\sum_{j,k,l} C_{jkl} q_j q_k q_l \tag{3}$$

$$+\epsilon^2 \sum_{j,k,l,m} C_{jklm} q_j q_k q_l q_m + \cdots = \sum_{n=1} \epsilon^n H_n(\mathbf{J},\mathbf{\Theta}). \tag{4}$$

Here, q_j and p_j are the jth normal coordinate and its conjugate momentum, respectively; ω_j and C_{jkl}, C_{jklm},... are, respectively, the frequency of the jth mode, the coupling coefficient among q_j, q_k, and q_l and that among q_j, q_k, q_l, and q_m, so forth. $\mathbf{J}$ and $\mathbf{\Theta}$ are, respectively, action and the conjugate angle variables of H_0, and ϵ is the strength of the perturbation. The frequency associated with an unstable reactive mode and those of the other stable modes are pure imaginary and real, respectively. In this paper, we focus on a $(3N-6)$-dof Hamiltonian system around a first-rank saddle with total linear and angular momenta of zero by eliminating the six degrees of freedom of the total translational and rotational motions.[39] To the regional Hamiltonians obtained by the expansion about stationary points, we apply a method to establish the coordinate system maximizing the local regularities in as many degrees of freedom as possible, so-called Lie canonical perturbation theory (LCPT),[43–46] among CPTs the most elaborate and sophisticated theory to achieve the transformation we seek.

To begin, let us see what all the several forms of CPTs provide. All the CPTs[42–46,52,53] require that the canonical transformation W of the coordinate system minimizes the angular dependencies of the new Hamiltonian $\overline{H}$, thereby making the new action variables $\overline{\mathbf{J}}$ as nearly constant as possible.[42] If the $\overline{H}$ can be obtained altogether independent of the angle $\overline{\mathbf{\Theta}}$ (at the order of the perturbative calculation performed), then

$$H(\mathbf{p},\mathbf{q}) \overset{W}{\rightarrow} \overline{H}(\overline{\mathbf{p}},\overline{\mathbf{q}})=\overline{H}(\overline{\mathbf{J}})=\sum_{n=0} \epsilon^n \overline{H}_n(\overline{\mathbf{J}}), \tag{5}$$

so the new action and angle variables for the kth mode are expressed as

$$\frac{d\overline{J}_k}{dt}=\dot{\overline{J}}_k=-\frac{\partial \overline{H}(\overline{\mathbf{J}})}{\partial \overline{\Theta}_k}=0, \tag{6}$$

$$\overline{J}_k=\text{constant}, \tag{7}$$

and

$$\dot{\overline{\Theta}}_k=\frac{\partial \overline{H}(\overline{\mathbf{J}})}{\partial \overline{J}_k}\equiv \overline{\omega}_k(\overline{\mathbf{J}})=\text{constant}, \tag{8}$$

$$\overline{\Theta}_k=\overline{\omega}_k(\overline{\mathbf{J}})t+\beta_k, \tag{9}$$

where β_k is the arbitrary initial phase factor of the kth mode. These yield the equations of motion[38] for the new coordinates $\overline{\mathbf{q}}(\mathbf{p},\mathbf{q})$ and momenta $\overline{\mathbf{p}}(\mathbf{p},\mathbf{q})$, to obey "$\overline{H}$":

$$\frac{d^2\overline{q}_k(\mathbf{p},\mathbf{q})}{dt^2}+\overline{\omega}_k^2 \overline{q}_k(\mathbf{p},\mathbf{q})=0 \tag{10}$$

and

$$\overline{p}_k(\mathbf{p},\mathbf{q})=\frac{\omega_k}{\overline{\omega}_k}\frac{d\overline{q}_k(\mathbf{p},\mathbf{q})}{dt}, \tag{11}$$

where $\overline{\omega}_k[=\overline{\omega}_k(\overline{\mathbf{J}})=\overline{\omega}_k(\overline{\mathbf{p}},\overline{\mathbf{q}})]$ is independent of time t because the $\overline{\mathbf{J}}$ are constant.

The advantage of any of the several forms of CPT is the reduction of dimensionality needed to describe the Hamiltonian, for instance, Eqs. (10) and (11) tell us that even though the motions look quite complicated in the old coordinate system, they could be followed as simple decoupled periodic orbits in the phase space, without any elaborate MD calculation. For realistic many-body nonlinear systems, Eqs. (10) and (11) may not be retained through the dynamical evolution of the system (even if the CPT calculation could extend to the global region of the system). This is because the (near-)commensurable conditions may densely distribute in typical regions throughout the phase space, that is, any integer linear combination of frequencies that vanishes identically at some order, ϵ^n, makes the corresponding new Hamiltonian diverge and destroys invariants of motion.[42] If the system satisfies any such (near-)commensurable condition, the new Hamiltonian must include the corresponding angle variables to avoid divergence.[48–50,53] Otherwise the CPT calculation would have to be performed to infinite order in cases of near-commensurability.

Up to now, most studies based on the CPTs have focused on transforming the new Hamiltonian itself to as simple a form as possible, to avoid divergence, and to obtain this form through specific CPT calculations of low finite order. A much more demanding usage of CPT, especially for many-body chemical reaction systems, should be its application as a detector to monitor occurrence of local invariance, by use of the new action $\overline{J}_k(\mathbf{p},\mathbf{q})$ and the new frequency $\overline{\omega}_k(\mathbf{p},\mathbf{q})$ along MD trajectories obeying equations of motion of the *original* Hamiltonian $H(\mathbf{p},\mathbf{q})$. That is, it is quite likely that the more dof in the system, the more the global invariants through the whole phase space become spoiled; nevertheless the invariants of motion might survive within a *certain locality*, i.e., for a certain finite duration, a region of phase space and/or in a certain limited subset of dof. The standard resonance Hamiltonian[53] constructed to avoid the near-commensurability might also eliminate the possibility of detecting such a limited, approximate invariant of motion retained in a certain locality.

The traditional Poincaré–Von Zeipel approach[42] of CPT is based on mixed-variable generating functions F:

$$\overline{\mathbf{q}}=\frac{\partial F(\overline{\mathbf{p}},\mathbf{q})}{\partial \overline{\mathbf{p}}}, \quad \mathbf{p}=\frac{\partial F(\overline{\mathbf{p}},\mathbf{q})}{\partial \mathbf{q}}, \tag{12}$$

which require functional inversion to obtain explicit formulas for $(\mathbf{p},\mathbf{q})$ in terms of $(\overline{\mathbf{p}},\overline{\mathbf{q}})$ and vice versa, at each order of the perturbative calculation. This imposes a major impediment to implementing higher-order perturbations and to treating systems with many degrees of freedom. With the mixed-variable generating functions, Gustavson[53] developed an elegant technique to extract the new Hamiltonian to avoid a divergence by assuming that the new Hamiltonian is expandable in normal form;[52] if the complete inversion of the variables is not required, the procedure to calculate the new Hamiltonian can be rather straightforward.

Lie canonical perturbation theories (LCPT),[43–46] first developed by Hori,[43,44] are superior to all the traditional methods, in that no cumbersome functions of mixed variables appear and all the terms in the series are repeating Poisson brackets. Lie transforms induce a canonical transformation, which can be regarded as a ''virtual'' time evolution of phase space variables $\mathbf{z}$ along the time ϵ driven by a ''Hamiltonian'' W, i.e.,

$$\frac{d\mathbf{z}}{d\epsilon}=\{\mathbf{z},W(\mathbf{z})\}\equiv -L_W\mathbf{z}. \tag{13}$$

Here, {} denotes the Poisson bracket. The formal solution can be represented as

$$\mathbf{z}(\epsilon)=\exp\left[-\int^{\epsilon}L_{W(\epsilon')}d\epsilon'\right]\mathbf{z}(0). \tag{14}$$

It can be easily proved,[43,46] for any transforms described by the functional form of Eq. (14), that if the $\mathbf{z}(0)$ are canonical, $\mathbf{z}(\epsilon)$ are also canonical (and vice versa), as the time evolution of any Hamiltonian system is regarded as a canonical transformation from canonical variables at an initial time to those at another time, withholding the structure of Hamilton's equations. For any function f evaluated at ''a point'' $\mathbf{z}(0)$, the evolution operator T yields a new function g represented as a function of $\mathbf{z}(0)$ and ϵ, whose functional *value* is equal to f evaluated at ''the other point'' $\mathbf{z}(\epsilon)$:

$$f(\mathbf{z}(\epsilon))=Tf(\mathbf{z}(0))=\exp\left[-\int^{\epsilon}L_{W(\mathbf{z}(0);\epsilon')}d\epsilon'\right]f(\mathbf{z}(0))$$
$$=g(\mathbf{z}(0);\epsilon). \tag{15}$$

The Lie transforms of an autonomous Hamiltonian H to a new Hamiltonian $\overline{H}$ can be brought about by

$$\overline{H}(\mathbf{z}(\epsilon))=T^{-1}H(\mathbf{z}(\epsilon))=H(\mathbf{z}(0)), \tag{16}$$

by determining the W (also assumed to be expandable in powers of ϵ as H and $\overline{H}$ are) so as to make the new Hamiltonian as free from the new angle variables $\overline{\mathbf{\Theta}}$ as possible, at each order in ϵ.[43–46] Here, the *inverse* evolution operator T^{-1} brings the system dwelling at a ''time'' backward to the past in ϵ from *that* time along the dynamical evolution of $\mathbf{z}$. yielding $H(\mathbf{z}(0))$. We shall hereinafter designate the initial values of $\mathbf{z}$, $\mathbf{z}(0)$, by $(\mathbf{p},\mathbf{q})$, and those at time ϵ by $(\overline{\mathbf{p}},\overline{\mathbf{q}})$ Then, one can see that Eq. (16) corresponds to a well-known relation between the old and new Hamiltonians hold under any canonical transformation for autonomous systems:

$$\overline{H}(\overline{\mathbf{p}},\overline{\mathbf{q}})=H(\mathbf{p},\mathbf{q}). \tag{17}$$

The great advantage of LCPT in comparison with Gustavson's normal form[53] is that, after the W is once established through each order, the new transformed physical quantities, e.g., new action $\overline{J_k}$, frequency $\overline{\omega_k}$, momentum $\overline{p_k}$, and coordinate $\overline{q_k}$ of the kth mode, can be expressed straightforwardly as functions of the original momenta and coordinates $(\mathbf{p},\mathbf{q})$ by using the evolution operator T,

$$\overline{J_k}(\mathbf{p},\mathbf{q})=TJ_k(\mathbf{p},\mathbf{q})=T\left(\frac{p_k^2+\omega_k^2q_k^2}{2\omega_k}\right), \tag{18}$$

$$\overline{\omega_k}(\mathbf{p},\mathbf{q})=T\frac{\partial\overline{H}}{\partial\overline{J_k}}, \tag{19}$$

$$\overline{p_k}(\mathbf{p},\mathbf{q})=Tp_k, \tag{20}$$

$$\overline{q_k}(\mathbf{p},\mathbf{q})=Tq_k. \tag{21}$$

For convenience, we denote hereinafter the transformed quantities in terms of $(\mathbf{p},\mathbf{q})$ by $\overline{f}(\mathbf{p},\mathbf{q})$, e.g., not $J_k(\mathbf{p},\mathbf{q})$ but $\overline{J_k}(\mathbf{p},\mathbf{q})$, because we have already used the notation, e.g., $J_k(\mathbf{p},\mathbf{q})$ to represent the action of H_0,

$$J_k(\mathbf{p},\mathbf{q})=\frac{p_k^2+\omega_k^2q_k^2}{2\omega_k}=\frac{1}{2\pi}\oint_{E=H_0(\mathbf{p},\mathbf{q})}p_kdq_k. \tag{22}$$

Note that the coordinates of the *original* system $\{p_k,q_k\}$ are, in other terms, regarded as the canonical variables to represent harmonic motions of H_0, but $\{\overline{p_k}(\mathbf{p},\mathbf{q}),\overline{q_k}(\mathbf{p},\mathbf{q})\}$ correspond to the canonical variables, which represent periodic/hyperbolic regular motions in the phase space for the nonlinear $H(\mathbf{p},\mathbf{q})$ if $\overline{H}(\overline{\mathbf{p}},\overline{\mathbf{q}})$ *actually* exists.

For practical calculations, we apply a so-called ''algebraic quantization,'' [37,48–50] which replaces the cumbersome analytical differentiation and integration calculations that appear in LCPT calculations carried out by computing directly with symbolic operations based on simple Poisson bracket rules. In the present article, we analyze the above physical quantities up to a finite, second order in ϵ, through which no commensurability conditions were encountered. For example, $\overline{p_k^{i\text{th}}}(\mathbf{p},\mathbf{q})$ and $\overline{q_k^{i\text{th}}}(\mathbf{p},\mathbf{q})$ have the following forms, respectively,

$$\overline{p_k^{i\text{th}}}(\mathbf{p},\mathbf{q})=\sum_{n=0}^{i}\sum_{j}\epsilon^nc_j^n\mathbf{p}^{2n_j-1}\mathbf{q}^{m_j}, \tag{23}$$

$$\overline{q_k^{i\text{th}}}(\mathbf{p},\mathbf{q})=\sum_{n=0}^{i}\sum_{j}\epsilon^nd_j^n\mathbf{p}^{2n'_j}\mathbf{q}^{m'_j}, \tag{24}$$

where, for example,

$$\mathbf{q}^{m_j}\equiv\prod_{l=1}^{M}q_l^{m_l}, \tag{25}$$

$$m_j=\sum_{l=1}^{M}m_l. \tag{26}$$

Each coefficient depends on the original Hamiltonian and the order of CPT. For example, c_j^n denotes the coefficient of the jth term at the $n(\leqslant i)$th order in $\overline{p_k^{i\text{th}}}(\mathbf{p},\mathbf{q},)$ n_j and $m_j(\geqslant 0)$ are arbitrary positive integers of $\mathbf{p},\mathbf{q}$ of the jth term at the

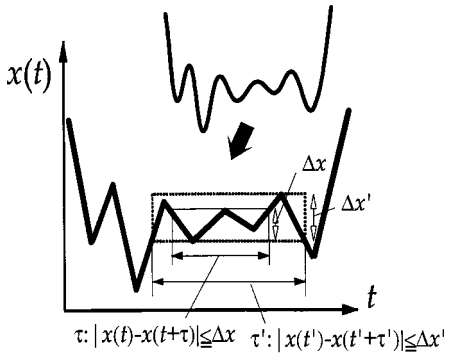

FIG. 1. Invariance analysis for a time-series of $x(t)$.

$n(<i)$th order in $\overline{p}_k^{i\text{th}}(\mathbf{p},\mathbf{q})$. The new $\overline{p}_k^{i\text{th}}(\mathbf{p},\mathbf{q})$ and $\overline{q}_k^{i\text{th}}(\mathbf{p},\mathbf{q})$ maintain time reversibility. We showed in the on-line supplement[39] the expressions through second order for $\overline{p_1}(\mathbf{p},\mathbf{q})$ and $\overline{q_1}(\mathbf{p},\mathbf{q})$ at saddle I, defined below, of Ar_6. The contributions of the original p_1 and q_1 in $\overline{p}_1^{i\text{th}}(\mathbf{p},\mathbf{q})$ and $\overline{q}_1^{i\text{th}}(\mathbf{p},\mathbf{q})$ are not necessarily large and almost all modes contribute to $\overline{p}_1^{i\text{th}}(\mathbf{p},\mathbf{q})$ and $\overline{q}_1^{i\text{th}}(\mathbf{p},\mathbf{q})$ for $i \geqslant 1$ (hereinafter, mode 1 denotes the reactive mode in this article).

III. LOCAL INVARIANCE ANALYSIS

Almost all studies based on CPT so far have worked to find constants of motion or good quantum numbers by transforming to a new, near-integrable form, particularly by transforming into as a simple form as possible. In our strategy, by monitoring the fluctuations of $\overline{J_k}(\mathbf{p},\mathbf{q})$ and/or $\overline{\omega_k}(\mathbf{p},\mathbf{q})$ along the *original* Hamiltonian dynamics, we scrutinize invariances of motions buried in the complexity of the original $H(\mathbf{p},\mathbf{q})$ without making any explicit assumption of the integrability of $H(\mathbf{p},\mathbf{q})$. Thus, in contrast to the standard usage of CPT, this monitoring-invariant procedure provides us with a clue of which parts of space (usually, phase space rather than configuration space) are those in which there are local or regional invariants of motion, which tend to persist during the course of dynamical evolution, e.g., during isomerizations, reactions or vibrational relaxations. Such surviving or vague invariancies in many-body systems occur, in general, only for certain finite durations and in certain limited dof, in contrast to the Kolmogorov-Arnold-Moser (KAM) tori whose dimension is exactly equal to the total number of dof.

Here, we introduce a concept of ''duration of regularity (τ).'' This is the residence time, for each mode of the system at each order of perturbation, for which each mode remains in the region of its near-constant action or frequency, as determined by a chosen bound on the fluctuation $\Delta\overline{J}$ or $\Delta\overline{\omega}$. As depicted in Fig. 1, we first transform a time series of the variables, denoted hereinafter as $x(t)$, to a sequence of stationary points, $\cdots$-min[i]-max[$i+1$]-min[$i+2$]-$\cdots$ along $x(t)$ with the corresponding times $t[i]$. By choosing all the possible combinations of max[i] and min[j], we calculate each residence τ for which $x(t)$ traverses each fluctuation window Δx defined as max[i]-min[j]. For a bundle of $x(t)$ one can calculate how frequently $x(t)$ traverses the region of a certain fluctuation window Δx for a certain τ, i.e., the residence probability $P_2(\Delta x;\tau)$

$$P_2(\Delta x;\tau)=\frac{N_2(\Delta x;\tau)}{\int d\Delta x d\tau N_2(\Delta x;\tau)}, \tag{27}$$

where $N_2(\Delta x;\tau)$ is the frequency of the time-evolution of $x(t)$ within Δx for time τ. Even if two independent evolutions of $x(t)$ has a same τ with a same Δx, the initial point in time t to measure τ would differ. Thus, if $x(t)$ is a physical quantity such as $\overline{J}_k^{i\text{th}}(\mathbf{p}(t),\mathbf{q}(t))$, the part of the phase space the system traverses while maintaining $x(t)$ nearly constant through τ would differ with each initial condition. Thus, we also calculated several distinct forms of joint probabilities, $P_{h+1}(\xi_1,\xi_2,\ldots,\xi_h;\tau)$ where ξ_i is either Δx, x, $\Delta x'$, or x' of any other variable $x'(t)$,x'/x is the short-term average of $x'(t)/x(t)$ for a certain period τ, say, from t' to $t'+\tau$, e.g.,

$$x' \equiv \frac{1}{\tau}\int_{t'}^{t'+\tau} dt x'(t). \tag{28}$$

To calculate the statistics and sample the regions of the time-series efficiently, we chose all the possible combinations of max[i] and min[j] calculated for every $x(t)$,$x'(t)$,..., if the ξ_i include more than one fluctuation bound, Δx,$\Delta x'$,..., by transforming each to each sequence of the set of stationary points to sample each bound Δx,$\Delta x'$,... . In practice, the integrals appeared in calculation, e.g., Eq. (27), are replaced as the summation for a calculated set of $\{\xi_i\}$ and τ. For example, as the $h=2$ joint probabilities, $P_3(\Delta\overline{J}_k^{i\text{th}},p_1;\tau)$ tells us how the passage velocity through the saddle, p_1, would influence the finite time(τ) quasi-invariant of action along mode k at ith order; and $P_3(\Delta\overline{J}_1^{2\text{nd}},\Delta\overline{\omega}_1^{2\text{nd}};\tau)$, how the system resides in both the quasi-invariants of action and frequency during the same time-evolution, say, from t' to $t'+\tau$ with the same period τ, along the reactive mode 1 at second order; as the $h=3$ joint probabilities, $P_4(\Delta\overline{J}_1^{2\text{nd}},\Delta\overline{\omega}_1^{2\text{nd}},p_1;\tau)$ tells us how the τ-residence of the system in both the quasi-invariant of $\overline{J}_1^{2\text{nd}}(\mathbf{p},\mathbf{q})$ and $\overline{\omega}_1^{2\text{nd}}(\mathbf{p},\mathbf{q})$ is affected by the passage velocity through the saddle; and $P_4(\Delta\overline{J}_1^{2\text{nd}},p_1,q_1;\tau)$, how the finite time ($\tau$) quasi-invariant action $\overline{J}_1^{2\text{nd}}(\mathbf{p},\mathbf{q})$ distributes in two-dimensional plane (p_1,q_1).

We also calculated the integrated quantities of P_{h+1} over all the calculated τ, $\overline{P}_{h+1}(\xi_1,\xi_2\ldots,\xi_h)$,

$$\overline{P}_{h+1}(\xi_1,\xi_2,\ldots,\xi_h)=\int d\tau P_{h+1}(\xi_1,\xi_2,\ldots,\xi_h;\tau). \tag{29}$$

We use $\overline{J}_k^{i\text{th}}(\mathbf{p}(t),\mathbf{q}(t))$, $\overline{\omega}_k^{i\text{th}}(\mathbf{p}(t),\mathbf{q}(t))$, $\overline{p}_k^{i\text{th}}(\mathbf{p}(t),\mathbf{q}(t))$, and $\overline{q}_k^{i\text{th}}(\mathbf{p}(t),\mathbf{q}(t))$ as $x(t)$,$x'(t)$... and calculate, in Sec. IV, several such joint probabilities in the region of the transition states, by using 10 000 ''well-saddle-well'' trajectories generated microcanonically. The analyses of local frequencies were done only at second order because of $\overline{\omega}_k^{i\text{th}}(\mathbf{p},\mathbf{q})=\omega_k$ = constant for $i=0$, and 1.

IV. MODEL AND CALCULATIONS

We have applied this method to saddle crossing dynamics in Ar_6, represented by the sum of pairwise Lennard-Jones potentials. This should be regarded as an illustrative vehicle, with no peculiar or specific mode(s). This system encounters

rather well representable situations in the regions of its transition states, compared with some chemical bond breaking-and-forming reactions.[37,38] We assign laboratory scales of energy and length appropriate for argon, i.e., $\varepsilon = 121\,\mathrm{K}$ and $\sigma = 3.4\,\text{Å}$ with the atomic mass $m = 39.948$ amu, and the total linear and angular momenta are set to zero.[39] This is the smallest inert gas cluster in which no saddle dynamics more regular than the dynamics within the local wells was revealed by the local K entropy analysis.[25] This cluster has two kinds of potential energy minima. The global minimum corresponds to an octahedral arrangement of the atoms (OCT), with energy $E = -12.712\varepsilon$, and the other, higher minimum, to a trigonal bipyramid structure of five atoms, capped on one face by the sixth atom (CTBP), with energy $E = -12.303\varepsilon$. There are two distinct kinds of first-rank saddles. One, saddle I, at energy $E = -12.079\varepsilon$ joins the OCT and the CTBP minima. The other higher saddle, saddle II, at energy $E = -11.630\varepsilon$, joins two permutationally distinct CTBP structures. Saddle II is slightly flatter than the lower saddle. See also the potential energy profile presented in Fig. 1 of our previous paper.[39] In the present study we mainly analyze the invariants of motion during the course of isomerization reaction, OCT⇌CTBP, at total energies $E = 0.1$, 0.5, and 1.0ε above the saddle point energy at saddle I, i.e., 16(45), 79(223), and 158(446)% of the barrier height of OCT→CTBP (OCT←CTBP). The computational recipe for constructing the $3N$-6(=12)-dof regional Hamiltonian was described elsewhere.[39] The three-, and four-body couplings terms for both the saddles are determined by introducing an appropriate cut-off value; the total number of terms is 106 three-, and 365 four-body couplings for saddle I.

Throughout this paper the parabolic barrier, the reaction coordinate in the original $(\mathbf{p},\mathbf{q})$ space (and in the new $(\overline{\mathbf{p}},\overline{\mathbf{q}})$ space) is denoted as $q_1(\overline{q_1})$ and the other bath coordinates, as $q_2, q_3, \ldots, q_{12}(\overline{q_2}, \overline{q_3}, \ldots, \overline{q_{12}})$ in order of increasing frequency, $\omega_2 \leqslant \omega_3, \ldots, \leqslant \omega_{12}(\overline{\omega_2} \leqslant \overline{\omega_3}, \ldots, \leqslant \overline{\omega_{12}})$. The units of energy, coordinate-space distance, momentum, action, frequency, temperature, mass and time are, respectively, ε, $m^{1/2}\sigma$, $m^{1/2}\sigma\,\mathrm{ps}^{-1}$, Kps, ps^{-1}, K, argon atomic mass and ps, unless otherwise noted.

For analyses of the infrequent saddle crossings, we employed a modified Keck–Anderson method[39] to generate the microcanonical ensemble of well-saddle-well trajectories. We generated 10 000 well-saddle-well trajectories for both the saddles, which were found to be enough to yield statistical convergence in calculating the transmission coefficients in terms of many-body phase-space dividing hypersurfaces $S(\overline{q_1}^{i\text{th}}(\mathbf{p},\mathbf{q}) = 0)$ $(i = 0,1,2)$ at $E = 0.1$, 0.5, 1.0ε above both the saddles. For the trajectory calculations we used a fourth-order Runge-Kutta method with adaptive step-size control.[54] The total energies in our MD calculations were conserved within $\pm 1 \times 10^{-6}\varepsilon$.

V. RESULTS AND DISCUSSIONS

First, let us look into how long the system resides in the near-invariants of action at each order during the course of the reactions. To begin, curves of $P_2(\Delta\overline{J_1}^{i\text{th}};\tau)$ in the region of saddle I are shown in Fig. 2, at each order, with $E = 0.1\varepsilon$. The higher the order of the LCPT calculation performed, the longer is the residence time of the near-invariant, as measured by small fluctuations in the actions. As seen in the residence probability of the system remaining the near-invariant of action of the reactive mode, $\Delta\overline{J_1}$, almost all of the 10 000 trajectories going through saddle I actually exhibit this variable as a near-invariant within a very narrow zone, $\sim \Delta\overline{J_1}^{2\text{nd}} \leqslant 0.05$, at the second order. (Remember that the individual trajectories have different values of the action, $\overline{J_1}^{2\text{nd}}(\mathbf{p},\mathbf{q})$, depending on the incident $\mathbf{p}$ and $\mathbf{q}$ going into the saddle region.)

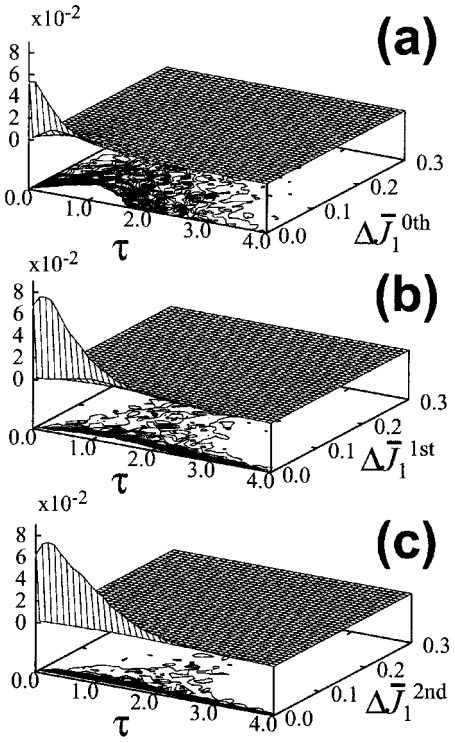

FIG. 2. The residence probabilities in the near-invariant of ith order action of reactive mode 1, $P_2(\Delta\overline{J_1}^{i\text{th}};\tau)$, in the region of saddle I at $E = 0.1\varepsilon$; (a) zeroth, (b) first, and (c) second order. The contours are drawn in the unit of 1/10 000 from 0 to 30/10 000, and the units of $\Delta\overline{J_1}^{i\text{th}}$ for mode 1 must be multiplied by a factor of an imaginary number i, throughout the following figures.

Then how does the system reside in each near-invariant of action associated with each mode, during the course of the reactions? Figure 3 shows the residence probabilities within a small region of the fluctuation of each action at each order at $E = 0.1\varepsilon$, for saddle I. Here, the width of the action fluctuation $\Delta\overline{J}$ was taken to be $\Delta\overline{J} \leqslant 0.05$; well-saddle-well trajectories, in all the most, reside in such a regime of $\Delta\overline{J_1}^{2\text{nd}}(\mathbf{p},\mathbf{q})$ along the reactive mode, at 0.1ε, where all the recrossing trajectories were rotated into single-crossing trajectories, in terms of the phase-space dividing hypersurface $S(\overline{q_1}^{2\text{nd}}(\mathbf{p},\mathbf{q}) = 0)$.[39] As only a small fluctuation in each action was allowed, the higher the order of the LCPT, the more almost all the actions become well-conserved along both reactive and nonreactive modes, i.e., at low energies, all trajectories become quasi-regular in almost of all dof, in the saddle region. In the zeroth order approximation (remember that the

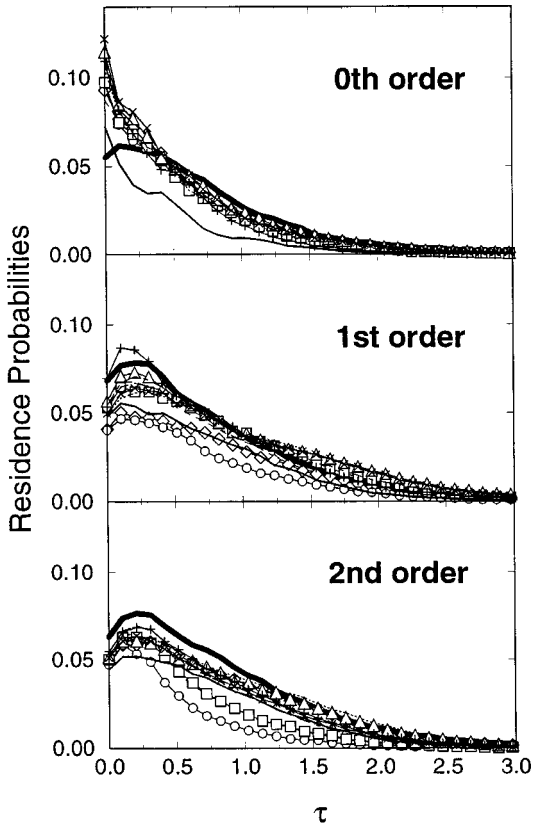

FIG. 3. The residence probabilities in the near-invariants of actions whose fluctuations $\Delta\overline{J}$ are within a small bound 0.05 at each order and each mode in the region of saddle I at $E=0.1\varepsilon$. The bold-solid line denotes reactive mode 1, and the other are the nonreactive; dashed, ◇, ○, □, dotted, long-dashed, △, ×, +, dot–dashed, and solid lines denote 2, 3, 4, 5, 6, 7, 8, 9, 10, 11, and 12, respectively.

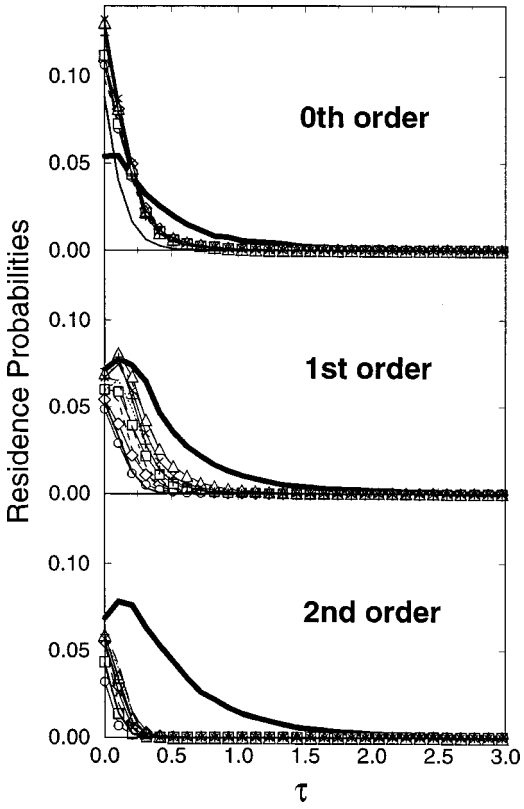

FIG. 4. The residence probabilities in the near-invariants of actions whose fluctuations $\Delta\overline{J}$ are within a small bound 0.05, at each order and each mode, in the region of saddle I at $E=0.5\varepsilon$. The meaning of each symbol is the same as in Fig. 3.

zeroth order means the trace of the functions of normal coordinates, in this case, action of H_0, along the original Hamiltonian dynamics), the escape rate of the system from the near-invariant of action, i.e., the inverse of residence time, is fastest on average along the fastest nonreactive mode 12, while the higher order calculation brings this mode down to make its fluctuations slower and more comparable to those of the other nonreactive modes.

How does the period of near-invariance of each mode's action change as the energy of the system increases? Intuition suggests, on the basis of behavior in the vicinity of potential energy minima, that the nonlinearities of the PES could not be considered as a ''sufficiently weak perturbation,'' as the energy of the system increases, and that the number of approximate local invariants should become smaller and smaller, going to zero at sufficiently high energy. (This is actually a statement of the so-called ''local equilibrium assumption'' that most reaction rate theories incorporate. This assumption is believed to hold at least for many-dof systems: The reaction system ergodically moves about, exploring the entire phase space domain of the reactant before crossing the transition state.) Figure 4 at $E=0.5\varepsilon$, 79% above of the saddle point energy from the OCT minimum, shows that the actions of nonreactive modes exhibit successively more variance and shorter durations of regularity as the calculation is refined to higher order. However, the higher the order of LCPT, the more the action in the mode of the reaction coordinate $\overline{J}_1$ stands out in bold relief as a near-constant of motion for longer and longer times. Despite the higher energy, the system retains its nearly invariant reactive-mode action through the saddle region with a residence probability within this fluctuation very similar to that at $E=0.1\varepsilon$. At much higher energy, $\sim 1.0\varepsilon$, the probability of the system retaining the invariants of action becomes much less even along the reaction coordinate at the second order, with an escape rate from that fluctuation band of the action much larger than those rates at lower energies.

In turn, how does the system reveal the degree of invariance of the frequency $\overline{\omega}_k(\mathbf{p},\mathbf{q})$ during the course of reactions? Figures 5 and 6 show, respectively, how long the frequency $\overline{\omega}_k^{2\mathrm{nd}}(\mathbf{p},\mathbf{q})$ dwells in three distinct regions of the fluctuation in the second-order frequency of each mode through saddle I, at $E=0.1\varepsilon$, and 0.5ε. The three distinct regions were taken to be $\Delta\overline{\omega}\leqslant\eta$, $\eta\leqslant\Delta\overline{\omega}\leqslant 2\eta$, and $2\eta\leqslant\Delta\overline{\omega}\leqslant 3\eta$, where η was such a fluctuation bound that the system reside within $\Delta\overline{\omega}_1(\equiv\Delta|\overline{\omega}_1|)\leqslant\eta$ for the (imaginary) frequency of reactive mode 1, at $E=0.1\varepsilon$. As Fig. 5 shows, most degrees of freedom exhibit almost complete near-invariance of frequency $\overline{\omega}_k^{2\mathrm{nd}}(\mathbf{p},\mathbf{q})$, within $\Delta\overline{\omega}\leqslant 0.02$, at $E=0.1\varepsilon$, just as in Fig. 3, although the frequencies for some modes, i.e., 2, 4, and 12, fluctuate a bit more than the others. At 0.5ε, the frequencies fluctuate more [see Figs. 6(b) and 6(c)] and a clear distinction appears among the frequency fluctuations in different modes. However, the one variable

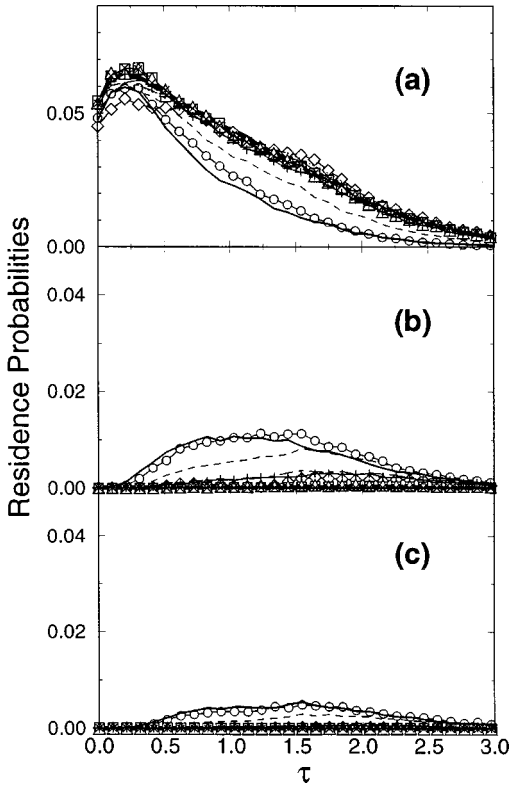

FIG. 5. The residence probabilities in the near-invariants of second-order frequencies $\bar{\omega}_k^{2\mathrm{nd}}(\mathbf{p},\mathbf{q})$ of each mode, whose fluctuations $\Delta\omega$ are; (a) $\Delta\bar{\omega} \leqslant 0.02$, (b) $0.02 \leqslant \Delta\bar{\omega} \leqslant 0.04$, and (c) $0.04 \leqslant \Delta\bar{\omega} \leqslant 0.06$, in the region of saddle I at $E=0.1\varepsilon$. The units of $\Delta\bar{\omega}_1^{2\mathrm{nd}}$ for mode 1 must be multiplied by a factor of an imaginary number i throughout the following figures. The meaning of each symbol is the same as in Fig. 3.

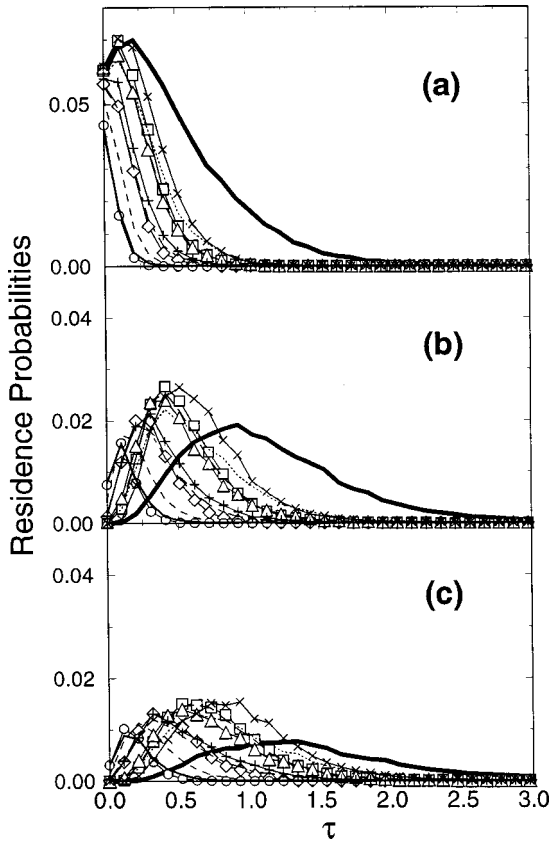

FIG. 6. The residence probabilities in the near-invariants of second-order frequencies $\bar{\omega}_k^{2\mathrm{nd}}(\mathbf{p},\mathbf{q})$ of each mode, whose fluctuations $\Delta\omega$ are; (a) $\Delta\bar{\omega} \leqslant 0.02$, (b) $0.02 \leqslant \Delta\bar{\omega} \leqslant 0.04$, and (c) $0.04 \leqslant \Delta\bar{\omega} \leqslant 0.06$, in the region of saddle I at $E=0.5\varepsilon$. The symbols are the same as in Fig. 5.

that stands out among all the rest is, again, the reaction coordinate $\bar{q}_1^{2\mathrm{nd}}$, whose frequency becomes more nearly constant than all the rest. At much higher energy, $\sim 1.0\varepsilon$, the fluctuations of the frequency along $\bar{q}_1^{2\mathrm{nd}}$ become more like those of the rest, and the residence probability distribution in the near-invariant band of the frequency develops a long tail toward large $\Delta\bar{\omega}_1$, like those distributions for the nonreactive modes.

Next, how do the invariances of both the action and the frequency correlate with each other along the reactive mode? The joint probability $\bar{P}_3(\Delta\bar{J}_1^{2\mathrm{nd}},\Delta\bar{\omega}_1^{2\mathrm{nd}})$ tells us how the system dwells in the regions of *both* the near-invariants of action and of frequency associated with $\bar{q}_1^{2\mathrm{nd}}$ for the *same* times. An example is that of Fig. 7, constructed at $E=0.5\varepsilon$ for passage over saddle I. Here, we found that, except for a very small τ, the topological shape of the joint probability distributions of P_3 we scrutinized in this article, $P_3(\Delta\bar{J}_1^{2\mathrm{nd}},\Delta\bar{\omega}_1^{2\mathrm{nd}};\tau)$ and the other P_3, are less influenced in τ, and look similar as the corresponding $\bar{P}_3$ integrated over τ. The figure shows that the smaller the fluctuation of $\bar{J}_1^{2\mathrm{nd}}(\mathbf{p},\mathbf{q})$, the smaller is the fluctuation of $\bar{\omega}_1^{2\mathrm{nd}}(\mathbf{p},\mathbf{q})$. Figure 8 shows how the passage velocity $|p_1|$ through the transition state influences to this; very slow passages manifestly spoil the invariance of $\bar{\omega}_1^{2\mathrm{nd}}(\mathbf{p},\mathbf{q})$ even while the action remains as an invariant of motion. In contrast, fast passages tend to make $\bar{\omega}_1^{2\mathrm{nd}}(\mathbf{p},\mathbf{q})$ remain rather constant. We expect that the slower the system passes through the transition state region at moderately high energies, where the system is manifestly chaotic, the more the system responds to significant nonlinearities of the PES due to its longer residence in that region. These nonlinearities would spoil any invariant of motion. This is, in fact, not the case because one of those quantities, action $\bar{J}_1^{2\mathrm{nd}}(\mathbf{p},\mathbf{q})$, remains as the near-invariant.

Let us look more deeply into this question by scrutinizing the other joint probability distributions at $E=0.5\varepsilon$ over saddle I. Figures 9 and 10 tell us where the system finds the near-invariant of action $\bar{J}_1^{2\mathrm{nd}}(\mathbf{p},\mathbf{q})$ and that of frequency

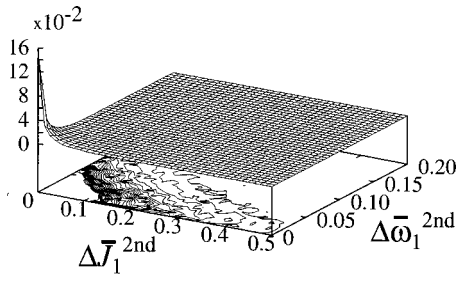

FIG. 7. The joint probability of residing in both the near-invariants of second-order action $\bar{J}_1^{2\mathrm{nd}}(\mathbf{p},\mathbf{q})$ and second-order frequency $\bar{\omega}_1^{2\mathrm{nd}}(\mathbf{p},\mathbf{q})$ of reactive mode 1, $\bar{P}_3(\Delta\bar{J}_1^{2\mathrm{nd}},\Delta\bar{\omega}_1^{2\mathrm{nd}})$, while the system is crossing saddle I at $E=0.5\varepsilon$. Here, $\bar{P}_3(\Delta\bar{J}_1^{2\mathrm{nd}},\Delta\bar{\omega}_1^{2\mathrm{nd}})$ is integrated the corresponding $P_3(\Delta\bar{J}_1^{2\mathrm{nd}},\Delta\bar{\omega}_1^{2\mathrm{nd}};\tau)$ over τ (see the text in detail).

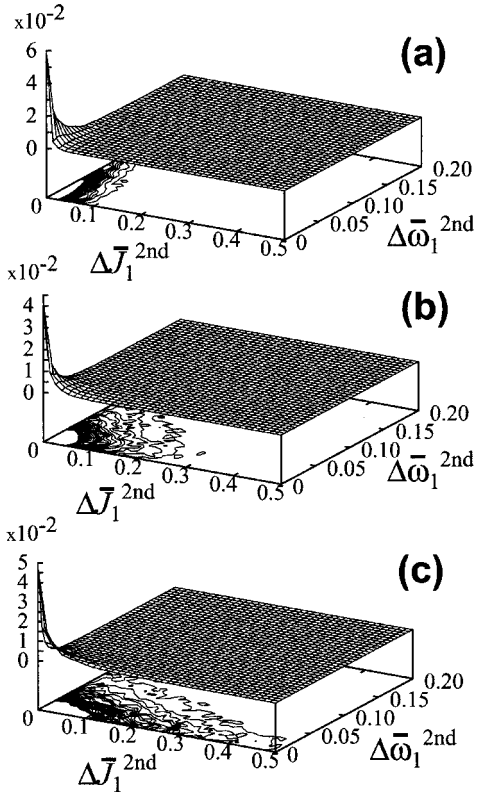

FIG. 8. The joint probability of residing in both the near-invariants of $\bar{J}_1^{2nd}(\mathbf{p},\mathbf{q})$ and $\bar{\omega}_1^{2nd}(\mathbf{p},\mathbf{q})$ as a function of the absolute value of passage velocity $p_1, \bar{P}_4(\Delta\bar{J}_1^{2nd}, \Delta\bar{\omega}_1^{2nd}, |p_1|)$, whose $|p_1|$ are; (a) $|p_1| \leqslant 0.02$, (b) $0.02 \leqslant |p_1| \leqslant 0.04$, and (c) $0.04 \leqslant |p_1| \leqslant 0.06$, in the region of saddle I at $E = 0.5\varepsilon$.

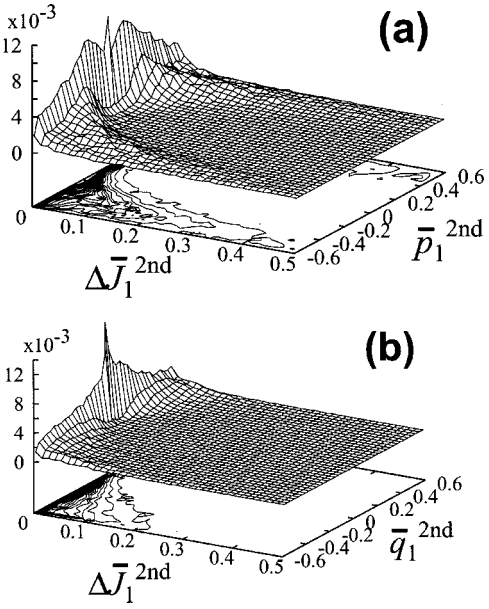

FIG. 9. The joint probabilities of how the system possesses $\bar{p}_1^{2nd}(\mathbf{p},\mathbf{q})$ and $\bar{q}_1^{2nd}(\mathbf{p},\mathbf{q})$ while residing in the near-invariant of second-order action $\bar{J}_1^{2nd}(\mathbf{p},\mathbf{q})$ in the region of saddle I at $E = 0.5\varepsilon$; (a) $\bar{P}_3(\Delta\bar{J}_1^{2nd}, \bar{p}_1^{2nd})$, (b) $\bar{P}_3(\Delta\bar{J}_1^{2nd}, \bar{q}_1^{2nd})$.

$\bar{\omega}_1^{2nd}(\mathbf{p},\mathbf{q})$ in terms of the reaction coordinate $\bar{q}_1^{2nd}(\mathbf{p},\mathbf{q})$, and the conjugate momentum $\bar{p}_1^{2nd}(\mathbf{p},\mathbf{q})$. As the figures show, the joint probabilities $\bar{P}_3(\Delta\bar{J}_1^{2nd}, \bar{p}_1^{2nd})$ and $\bar{P}_3(\Delta\bar{\omega}_1^{2nd}, \bar{p}_1^{2nd})$ indicate that the system establishes its near-invariant action, say, $\Delta\bar{J} \leqslant 0.05$, as the system slows through the transition state region, while, on the contrary, that slow transit of the system through the saddle does not establish the frequency as a near-invariant, for example to have variance $\Delta\bar{\omega}_1^{2nd} \leqslant 0.02$, in the local frequency space [see Figs. 9(a) and 10(a)]. In the regions further from $\bar{p}_1^{2nd} \approx 0$ in the distributions, the probabilities increase for the system to exhibit large fluctuations in both $\bar{J}_1^{2nd}(\mathbf{p},\mathbf{q})$ and $\bar{\omega}_1^{2nd}(\mathbf{p},\mathbf{q})$. This is simply due to the fact that, along the negatively curved reaction coordinate, the further the system moves from the bottleneck region of $\bar{q}_1^{i\text{th}} \approx 0$ $(i \geqslant 0)$, the larger is the $|\bar{p}_1^{i\text{th}}|$, thus yielding a large nonlinear effect associated with $\bar{q}_1^{i\text{th}}$. (This makes it difficult to treat the dynamics well away from the saddle via a finite perturbation calculation.) Note, however, that the near-invariance of $\bar{\omega}_1^{2nd}(\mathbf{p},\mathbf{q})$ in its region of very small fluctuations is well established even when $|\bar{p}_1^{2nd}|$ is large, compared with that of $\bar{J}_1^{2nd}(\mathbf{p},\mathbf{q})$ [see Figs. 9(a) and 10(a)]. The probability distributions in the reaction coordinate $\bar{q}_1^{2nd}(\mathbf{p},\mathbf{q})$, as shown in Figs. 9(b) and 10(b), imply that the well-conserved invariant in both the action and the frequency is located more in the vicinity of $\bar{q}_1^{2nd} \cong 0$ than in more distant regions. We found that the qualitative shapes of these joint probability distributions in terms of $\bar{p}_1^{2nd}(\mathbf{p},\mathbf{q})$ and $\bar{q}_1^{2nd}(\mathbf{p},\mathbf{q})$ look similar to those of p_1 and q_1, except that significantly more of probabilities for both $\Delta\bar{J}_1^{2nd}$ and $\Delta\bar{\omega}_1^{2nd}$, are localized around $p_1 \approx q_1 \approx 0$ as sharp peaks in their near-invariant regimes, in comparison with $\bar{p}_1^{2nd}(\mathbf{p},\mathbf{q}) \approx \bar{q}_1^{2nd}(\mathbf{p},\mathbf{q}) \approx 0$.

What mechanics underlies the clear distinction between invariances of action $\bar{J}_1^{2nd}(\mathbf{p},\mathbf{q})$ and of frequency $\bar{\omega}_1^{2nd}(\mathbf{p},\mathbf{q})$

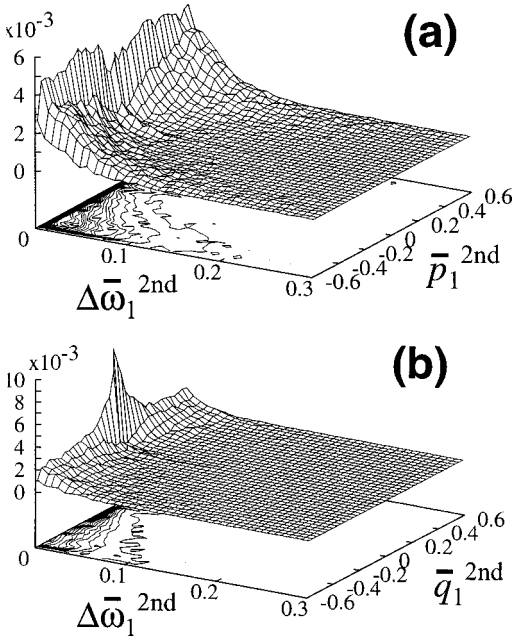

FIG. 10. The joint probabilities of how the system possesses $\bar{p}_1^{2nd}(\mathbf{p},\mathbf{q})$ and $\bar{q}_1^{2nd}(\mathbf{p},\mathbf{q})$ while residing in the near-invariant of second-order frequency $\bar{\omega}_1^{2nd}(\mathbf{p},\mathbf{q})$ in the region of saddle I at $E = 0.5\varepsilon$; (a) $\bar{P}_3(\Delta\bar{\omega}_1^{2nd}, \bar{p}_1^{2nd})$, (b) $\bar{P}_3(\Delta\bar{\omega}_1^{2nd}, \bar{q}_1^{2nd})$.

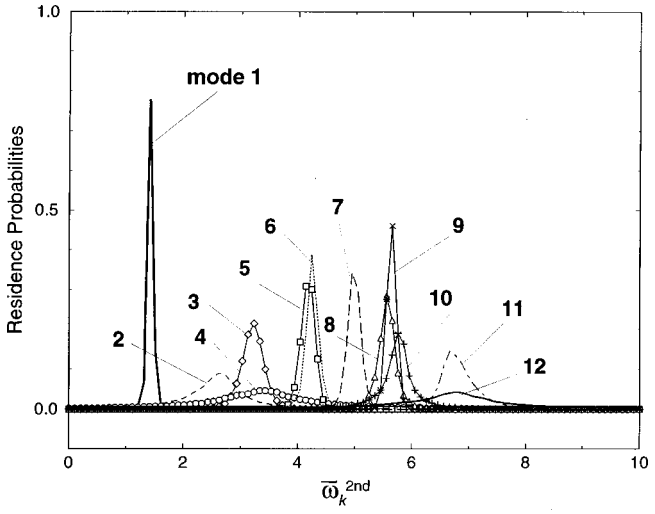

FIG. 11. The residence probabilities of the second-order frequencies $\bar{\omega}_k^{2nd}(\mathbf{p},\mathbf{q})$, $\bar{P}_2(\bar{\omega}_k^{2nd})$, in the region of saddle I at $E=0.5\varepsilon$, showing how the system possesses the near-constants of $\bar{\omega}_k^{2nd}(\mathbf{p},\mathbf{q})$. The meaning of each symbol is the same as in Fig. 3, and the unit of $\bar{\omega}_1^{2nd}$ must be multiplied by a factor of $-i$.

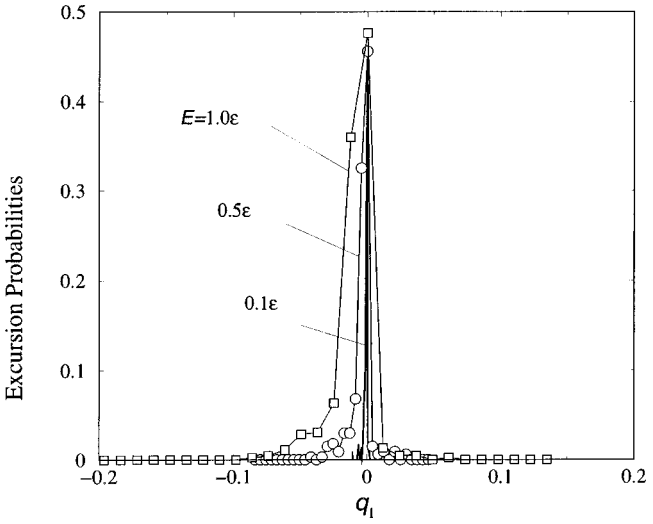

FIG. 12. The excursion length probabilities at $E=0.1$, 0.5, and 1.0ε in the region of saddle I (see the text in detail). The bold-solid, circle, and square lines denote 0.1, 0.5, and 1.0ε, respectively.

along the reaction coordinate $\bar{q}_1^{ith}(\mathbf{p},\mathbf{q})$? Especially, why do these near-invariances depend on the velocity of passage through the transition state? (We found that no such clear distinction appears at low energy, e.g., $E=0.1\varepsilon$.) The answer is this: The invariance of action associated with the reactive coordinate $\bar{q}_1(\mathbf{p},\mathbf{q})$ arises from the generic feature inherent in the region of (first-rank) saddle at the transition state, irrespective of the system; no arbitrary combination of modes can satisfy commensurable conditions to make an unstable mode mix with modes stable in that region, because one frequency ω_1 is pure-imaginary along the reactive dof and all the rest are real in the nonreactive dof.[39,40] On the contrary, the invariance of the local frequency $\bar{\omega}_1(\mathbf{p},\mathbf{q})$ might arise from ''adiabaticity'' of the passage through the transition state region, that is, passage fast enough to make the influence of the (individual) variations of the composite actions $\bar{J}_k$ in $\bar{\omega}_1(\bar{\mathbf{J}}(\mathbf{p},\mathbf{q}))$ less important if the system is not in the quasi-regular regime where all or almost of all the actions are ''good'' approximate invariants. We might still expect any nonconstancy of $\bar{\omega}_1$ to leave the separability of $\bar{q}_1$ as unaffected as $\bar{J}_1$ in the transition state. The reason is that to pass through a dividing surface from the one side to the other, the crossing trajectories typically require, at most, only a half period of the reactive hyperbolic orbit $\sim\pi/\bar{\omega}_1$; except through very flat saddles, the fluctuation of $\bar{\omega}_1$ should have little influence during such short time intervals, as shown in Fig. 11, $\bar{\omega}_1^{2nd}$ exhibits near-constant around $\bar{\omega}_1^{0th}(=\omega_1=-1.477i)$ with a fluctuation $\sim\pm 0.2i$, at 0.5ε through saddle I.

Local invariant of action $\bar{J}_1(\mathbf{p},\mathbf{q})$ in the original space and its energy dependence

How and where does the invariant of action distribute in the original phase space ($\mathbf{p}$, $\mathbf{q}$) and how is this regularity ruined in the region of the transition state with sufficiently high total energy? First, to show how the system traverses the transition state region before being captured in either of the stable states, we examine the probability distribution of excursion lengths Δq_1^{ex}, defined[55] as the maximum distance attained in the coordinate q_1 away from the barrier top, $q_1=0$, before returning to it; i.e., how extended is the region of recrossings? We explore this at $E=0.1$, 0.5, and 1.0ε through saddle I. Figure 12 shows that the more energy in the system, the longer are the returning excursions from the barrier top. The system more frequently traverses the minus side than the plus side of q_1 in the unsymmetrical saddle I before the system eventually goes into either of the stable states. As visualized before,[40,41] this is because the real, many-body phase space reaction bottleneck, defined as $S(\bar{q}_1^{2nd}(\mathbf{p},\mathbf{q})=0)$, is located in a region removed from $q_1=0$ to the minus of q_1 toward the global minimum OCT.

Now let us turn to the local invariant regime in the original space (p_1,q_1), and examine $P_4(\Delta\bar{J}_1^{2nd},p_1,q_1;\tau)$. Figure 13 shows how frequently the system passes through saddle I in the (p_1,q_1) plane, at $E=0.1$, 0.5, and 1.0ε, while it resides in the zone of its near-invariant action, ca. $\Delta\bar{J}_1^{2nd}\leqslant 0.05$, for a duration $\tau\geqslant 0.5$.[56] As described in our short report related to this article,[51] a large amount of cone-type invariant distributions occur in the hyperplane of the nonreactive dofs, e.g., $(\bar{p}_2^{2nd},\bar{q}_2^{2nd})$, at just slightly above the threshold, $\sim 0.1\varepsilon$. As the energy increases, say, $\geqslant 0.5\varepsilon$, such regions totally disappear. As seen in Fig. 13, in the reactive plane, the more the energy increases, the more the zone of invariant action shrinks toward the regime where $q_1\cong p_1\cong 0$ and the more the population of systems occupying the zone of near-invariance of action decreases (see the vertical axis). However, even at $E=0.5\varepsilon$, one can still see a much more significant amount of local regularity in the reactive space than in the nonreactive space. Much higher energy, $\sim E=1.0\varepsilon$, seemingly washes out the regularity even along the reaction mode, shrinking it toward the origin in that coordinate. Nonetheless, rather ''long-lived'' regularities around the origin, $p_1\cong q_1\cong 0$, emerge as the energy in-

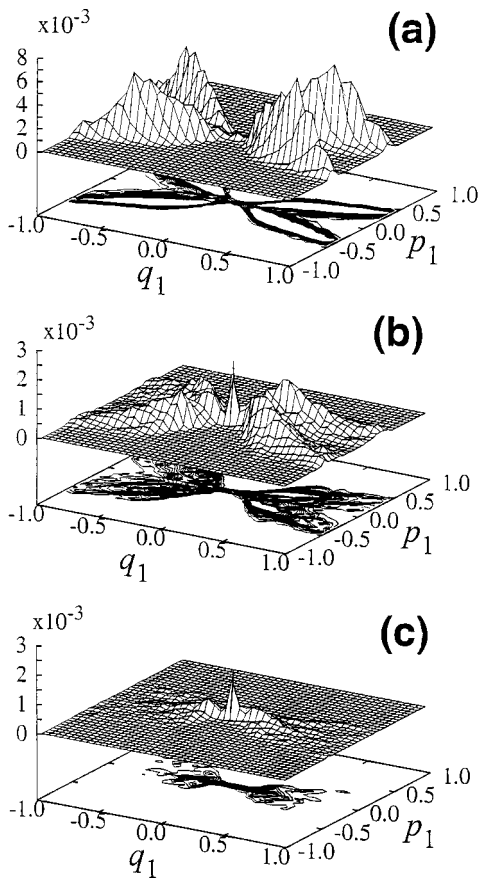

FIG. 13. The joint probabilities of the system residing in the near-invariant of the second-order action $\overline{J}_1^{2\mathrm{nd}}(\mathbf{p},\mathbf{q})$ whose fluctuations $\Delta\overline{J}$ are within a small bound 0.05 and whose duration τ is larger than 0.5, projected onto the two-dimensional (p_1,q_1) plane, at; (a) $E=0.1\varepsilon$, (b) $E=0.5\varepsilon$, (c) $E=1.0\varepsilon$ in the region of saddle I.

creases, even surviving to 1.0ε. This is irrespective of the higher incident passage velocity p_1 inferred from the higher energy, going through the reaction bottleneck. Such a ''long-lived'' regularity could not be observed in the quasi-regular region, 0.1ε.

Let us now interpret all the findings we have shown so far, in terms of the extent these are related to kinetics and reaction dynamics. The heavy, localized, and persistent weight of the distribution of near-invariants of $\overline{J}_1(\mathbf{p},\mathbf{q})$ and its associated $\overline{\omega}_1(\mathbf{p},\mathbf{q})$, up to moderately high energies, (see Figs. 2–6), implies that $\overline{p}_1(\mathbf{p},\mathbf{q})$ and $\overline{q}_1(\mathbf{p},\mathbf{q})$ are approximately decoupled from the other modes, and represent the local dynamics analytically. These observations strongly support the existence of a multidimensional dividing hypersurface in the phase space, defined by the condition that the reactive coordinate in the transformed coordinates is zero, and that this surface is free from recrossing problems.[39] The higher the energy of the system, the more distant are the returns of the recrossing trajectories from the barrier top (before going into either the reactant or product state) (see Fig. 12) while the more the region of the local-invariant of action $\overline{J}_1(\mathbf{p},\mathbf{q})$ shrinks (see Fig. 13). That is, the more the total energy increases, the more the broadening of the excursion regime competes with the shrinkage of the region of local invariance of the action, in which the reaction coordinate $\overline{q}_1$ decouples from the others. The outcome of this competition is retaining $\overline{q}_1(\mathbf{p},\mathbf{q})$ as a ''true reaction path'' along which the recrossing problem never appears essential.

Next, what is the implication of the sharpness of the distribution of the local invariant of action $\overline{J}_1^{2\mathrm{nd}}(\mathbf{p},\mathbf{q})$ in the context of reaction dynamics? This spike appears and persists in the region of $p_1\cong q_1\cong 0$, with an increase of the total energy of the system. Note that such a sharp spike around the origin can also be observed by the projection onto the $(\overline{p}_1^{2\mathrm{nd}},\overline{q}_1^{2\mathrm{nd}})$ plane,[51] and, even irrespective of the local invariance, in an integrated distribution of $\overline{P}_4(\Delta\overline{J}_1^{2\mathrm{nd}},p_1,q_1)$ over $\Delta\overline{J}_1^{2\mathrm{nd}}$. This implies that the system is ''trapped'' in the nonreactive space for a significant period during the course of the reaction. The appearance of such trapped trajectories at high energies implies that, with increasing total energy of the system, another type of bottleneck emerges in the energy flow between the reactive mode $\overline{q}_1(\mathbf{p},\mathbf{q})$ and the others. It would be almost impossible to distinguish between two possible origins this long-lived trapping phenomena, either (1) the space in which one views these, i.e., the order of the CPT calculation, since the trapping in phase space $[\overline{p}_1^{\infty\mathrm{th}}(\mathbf{p},\mathbf{q}),\overline{q}_1^{\infty\mathrm{th}}(\mathbf{p},\mathbf{q})]$ might be rotated away as no-trapping trajectories, or (2) the shrinkage of the convergence radius of CPT (even if an infinite-order CPT would be possible) within which the couplings among the reactive and nonreactive dofs are very weak. The reactive dof $\overline{q}_1^{i\mathrm{th}}(\mathbf{p},\mathbf{q})$ becomes coupled, as the energy of the system increases, with the other nonreactive dofs, not via ''resonances,'' but via straightforward nonlinear couplings, either from the higher orders $\geqslant O(\epsilon^{i+1})$ above the order at which one performed the CPT, or from those nonlinearities originating outside of the convergence radius. These kinds of trapping phenomena in the nonreactive space are, whatever the reason, quite generic irrespective of the system and the order of CPT we used, and should be the fundamental causes spoiling the invariance of frequency $\overline{\omega}_1$ even along the reactive coordinate $\overline{q}_1$, as observed while $|\overline{p}_1^{2\mathrm{nd}}(\mathbf{p},\mathbf{q})|$ is small [see Fig. 10(a)]. That is, long intervals with much energy stored in the nonreactive dofs could make the fluctuations of action of those modes affect the near-invariance of $\overline{\omega}_1(\overline{\mathbf{J}})$. Note here that, this suggests a previously-unrecognized type of phase space bottleneck in the energy flows among reactive dof and nonreactive dofs. At moderate to high energies, such bottlenecks may break the simplistic picture, ballistic or diffusive, of the system's passage through transition states, and even the microcanonical statistics (in the sense of requiring pathologically long time intervals to establish those statistics), though microcanonical statistics may be established quickly outside the region of the transition state.

At energies just slightly above the threshold, $\sim 0.1\varepsilon$, a similar sharp spike was detected around $\overline{p}_1^{2\mathrm{nd}}(\mathbf{p},\mathbf{q})\cong\overline{q}_1^{2\mathrm{nd}}(\mathbf{p},\mathbf{q})\cong 0$, but with much shorter residence time ($\tau\ll 0.3$ with the same fluctuation in its action). This finding implies that the original Hamiltonian can not be transformed to an exact, integrable Hamiltonian at second order of LCPT in the real situation at $E=0.1\varepsilon$. However, as shown in Fig. 3, almost of all the actions in the nonreactive space are re-

tained approximately as ''good'' invariants at that energy. The shorter trapping period, i.e., the fast energy flow between the nonreactive subspace and the reactive mode, suggests that trapping is brief in the apparently near-integrable part of the nonreactive space, and has less influence on the kinetics than the nonreactive modes in the chaotic subset. Remember that the standard Rice–Ramsperger–Kassel–Marcus (RRKM) theory[4–6] postulates that the greater the number of coupled dof, the slower is the energy concentration into a specific mode.

We also want to point out here what else the distributions show us, besides the sharp peak around its origin, of $P_4(\Delta\overline{J}_1^{2\mathrm{nd}},p_1,q_1;\tau)$ and $P_4(\Delta\overline{J}_1^{2\mathrm{nd}},\overline{p}_1^{2\mathrm{nd}},\overline{q}_1^{2\mathrm{nd}};\tau)$ (Fig. 5 in our short report[51]). In particular, the latter projections onto the new coordinate $\overline{q}_1^{2\mathrm{nd}}(\mathbf{p},\mathbf{q})$ and its conjugate momentum $\overline{p}_1^{2\mathrm{nd}}(\mathbf{p},\mathbf{q})$ clearly form an ''X''-character in the two-dimensional contour maps at all the three energies, just as stable and unstable manifolds to and from a hyperbolic point of a one-dimensional pendulum do. The projections onto the original space (p_1,q_1) form rather a vague ''X'' only at just slightly above the threshold, $\sim 0.1\varepsilon$. The reduction of dimensionality in the context of reaction dynamics has been one of the most outstanding subjects, e.g., for the control theory of chemical reaction dynamics.[57] This indicates that, without any (explicit) assumption of the separation of time scale associated with individual modes of the system, one can extract and visualize the stable, and unstable invariant manifolds, at least in the region of the transition state, along the decoupled reactive coordinate $\overline{q}_1(\mathbf{p},\mathbf{q})$ in the phase space.

VI. CONCLUDING REMARKS

We proposed the analyses of the local invariants in transition state regions via LCPT along the dynamics of the original Hamiltonian $H(\mathbf{p},\mathbf{q})$. In the present article, we have studied the invariances of local climb-and-go-through dynamics in the vicinity of the transition state. The results of this investigation provide a foundation for our previous conjecture,[39–41] the existence of at least three distinct energy ranges of dynamical behavior in the vicinities of (first-rank) transition states. These ranges are associated with the invariants of motion along the reactive coordinate $\overline{q}_1(\mathbf{p},\mathbf{q})$ in the phase space. This is, as Hernandez and Miller pointed out,[58] because any arbitrary combination of modes cannot satisfy commensurability conditions to make an unstable mode mix with modes stable in that region. Thus, this feature is generic for (first-rank) transition states irrespective of the system. Related to this, our approach provides us with a new, untouched, problem, e.g., what is the role of resonance in the imaginary ω-plane for the bifurcation? This is one of the most exciting questions, especially for relaxation dynamics on a rugged PES, if the system finds higher-rank saddles, which may be densely distributed in the regions of high potential energies, and would pass through such complicated regions at least as frequently as through the lowest reach, first-rank transition states. This will require going back to the fundamental question of what the transition state is, i.e., whether a dividing hypersurface could still exist or be definable, in terms of separating the space of the system into regions identifiable with individual stable states. The next forthcoming problem, inherent to the standard CPT so far, is determining how one can extend CPT to a global region of nonstationary points removed from the unstable fixed points. A recent development by Sugny and Joyeux[59] on selecting good zeroth-order Hamiltonians for floppy molecules, might be one of the candidates to address this problem.

In the present article, we focused mainly on the approximate invariants of motion associated with the reaction coordinate $\overline{q}_1$ and its ''statistical'' properties as expressed by joint probability distributions. The results strongly support the use of the concept of single, nearly separable reactive degrees of freedom in the system's phase space, degrees of freedom that are as free as possible from coupling to all the rest of the degrees of freedom. On the other hand, such statistical analyses with no other analytical tools would spoil the possibility of detecting the dynamical nonuniformity[15–18] buried among ''nonreactive'' dofs, which should become more crucial as the system size decreases. As yet, there is no general answer as to whether a dynamical bottleneck even exists in the reactant phase space domain for large systems, say, >10 dof. Along this direction, although we only showed how the ''invariant'' of frequency arises, varying the ratios of frequencies $\overline{\omega}_k$ among the modes should shed light on what kinds of energy flows take place among $\overline{q}_k(\mathbf{p},\mathbf{q})$ space.[60–62] Obviously, the more the dof, the more possible combinations emerge to make the system complicated.

Besides the recrossing problem, the remaining ambiguity in many chemical reaction theories is the assumption of local vibrational equilibrium: In a strong form, this becomes the assumption that the reactant and the system in the transition state move ergodically, exploring all the phase space of the reactant domain before crossing the transition state. (In a weaker form, one assumes only that the vibrational energy is equipartitioned in the reactant and in the transition state.) One possible diagnosis to look deeply into this question in many-dof systems would be to execute the backward trajectory calculation, starting on the phase-space dividing hypersurface $S(\overline{q}_1(\mathbf{p},\mathbf{q})=0)$, sampled from the microcanonical ensemble. If the system exhibits an invariant of motion for a certain time in the reactant phase space, that is, if the system is trapped in a certain limited region for some period, this analysis should tell us how the local-equilibrium assumption is violated in the reaction. The backward calculations initiated with large momenta $\overline{p}_1(\mathbf{p},\mathbf{q})$ on the LCPT dividing hypersurface, i.e., the bundle of the fast transitions from the reactant to product if one inverts the time, would reveal how any mode-specific nature of a reaction relates with the local topography of the phase space in the reactant state. With these, we have reviewed some of the open subjects that remain ahead in statistical theories of many-dof systems.

ACKNOWLEDGMENTS

The authors thank Professors Stuart Rice, William Miller, Mikito Toda, and Stephen Gray for their valuable, stimulating discussions. One of the authors (T.K.) expresses his gratitude to Professor Rice and Dr. M. Zhao for their warm hospitality at The James Franck Institute during his short-term stay. This research was supported by the National

Science Foundation, the Japan Society for the Promotion of Science, and The Ministry of Education, Science, Sports and Culture in Japan.

[1] H. Eyring, J. Chem. Phys. **3**, 107 (1935).
[2] M. G. Evans and M. Polanyi, Trans. Faraday Soc. **31**, 875 (1935).
[3] E. Wigner, J. Chem. Phys. **5**, 720 (1938).
[4] O. K. Rice and H. C. Ramsperger, J. Am. Chem. Soc. **50**, 617 (1928).
[5] L. S. Kassel, J. Phys. Chem. **32**, 1065 (1928).
[6] R. A. Marcus, J. Chem. Phys. **20**, 359 (1952).
[7] J. C. Keck, Adv. Chem. Phys. **13**, 85 (1967).
[8] D. G. Truhlar and B. C. Garrett, Acc. Chem. Res. **13**, 440 (1980).
[9] H. A. Kramers, Physica (Amsterdam) **7**, 284 (1940).
[10] J. T. Hynes, in *Theory of Chemical Reaction Dynamics*, edited by M. Baer (CRC, Boca Raton, 1985), pp. 171–234.
[11] W. H. Miller, Faraday Discuss. Chem. Soc. **62**, 40 (1977).
[12] T. Seideman and W. H. Miller, J. Chem. Phys. **95**, 1768 (1991).
[13] B. J. Berne, M. Borkovec, and J. E. Straub, J. Phys. Chem. **92**, 3711 (1988).
[14] D. G. Truhlar, B. C. Garrett, and S. J. Klippenstein, J. Phys. Chem. **100**, 12771 (1996).
[15] M. J. Davis and S. K. Gray, J. Chem. Phys. **84**, 5389 (1986).
[16] S. K. Gray and S. A. Rice, J. Chem. Phys. **87**, 2051 (1987).
[17] M. Zhao and S. A. Rice, J. Chem. Phys. **96**, 6654 (1992).
[18] R. E. Gillilan and G. S. Ezra, J. Chem. Phys. **94**, 2648 (1991).
[19] N. De Leon, M. A. Mehta, and R. Q. Topper, J. Chem. Phys. **94**, 8310 (1991); **94**, 8329 (1991); N. De Leon, *ibid.* **96**, 285 (1992).
[20] J. R. Fair, K. R. Wright, and J. S. Hutchinson, J. Phys. Chem. **99**, 14707 (1995).
[21] T. L. Beck, D. M. Leitner, and R. S. Berry, J. Chem. Phys. **89**, 1681 (1988).
[22] D. J. Wales and R. S. Berry, J. Phys. B **24**, L351 (1991).
[23] R. J. Hinde, R. S. Berry, and D. J. Wales, J. Chem. Phys. **96**, 1376 (1992).
[24] C. Amitrano and R. S. Berry, Phys. Rev. Lett. **68**, 729 (1992); Phys. Rev. E **47**, 3158 (1993).
[25] R. J. Hinde and R. S. Berry, J. Chem. Phys. **99**, 2942 (1993).
[26] R. S. Berry, Chem. Rev. **93**, 237 (1993).
[27] R. S. Berry, Int. J. Quantum Chem. **58**, 657 (1996).
[28] S. K. Nayak, P. Jena, K. D. Ball, and R. S. Berry, J. Chem. Phys. **108**, 234 (1998).
[29] E. R. Lovejoy, S. K. Kim, and C. B. Moore, Science **256**, 1541 (1992).
[30] E. R. Lovejoy and C. B. Moore, J. Chem. Phys. **98**, 7846 (1993).
[31] D. C. Chatfield, R. S. Friedman, D. G. Truhlar, B. C. Garrett, and D. W. Schwenke, J. Am. Chem. Soc. **113**, 486 (1991).
[32] R. A. Marcus, Science **256**, 1523 (1992).
[33] S. Wiggins, *Normally Hyperbolic Invariant Manifolds in Dynamical Systems* (Springer-Verlag, New York, 1991).
[34] M. Toda, Phys. Rev. Lett. **74**, 2670 (1995).
[35] M. Toda, Phys. Lett. A **227**, 232 (1997).
[36] P. Pechukas and E. Pollak, J. Chem. Phys. **67**, 5976 (1977): E. Pollak and P. Pechukas, *ibid.* **69**, 1218 (1978); **70**, 325 (1979): E. Pollak, M. S. Child, and P. Pechukas, *ibid.* **72**, 1669 (1980): M. S. Child and E. Pollak, *ibid.* **73**, 4365 (1980).
[37] T. Komatsuzaki and M. Nagaoka, J. Chem. Phys. **105**, 10838 (1996).
[38] T. Komatsuzaki and M. Nagaoka, Chem. Phys. Lett. **265**, 91 (1997).
[39] T. Komatsuzaki and R. S. Berry, J. Chem. Phys. **105**, 10838 (1999).
[40] T. Komatsuzaki and R. S. Berry, Phys. Chem. Chem. Phys. **1**, 1387 (1999).
[41] T. Komatsuzaki and R. S. Berry, J. Mol. Struct.: THEOCHEM **506**, 55 (2000).
[42] A. J. Lichtenberg and M. A. Lieberman, *Regular and Chaotic Dynamics*, 2nd ed. (Springer, New York, 1992).
[43] G. Hori, Publ. Astron. Soc. Jpn. **18**, 287 (1966).
[44] G. Hori, Publ. Astron. Soc. Jpn. **19**, 229 (1967).
[45] A. Deprit, Celest. Mech. **1**, 12 (1969).
[46] A. J. Dragt and J. M. Finn, J. Math. Phys. **17**, 2215 (1976); **20**, 2649 (1979).
[47] J. R. Cary, Phys. Rep. **79**, 130 (1981).
[48] L. E. Fried and G. S. Ezra, J. Chem. Phys. **86**, 6270 (1987).
[49] L. E. Fried and G. S. Ezra, Comput. Phys. Commun. **51**, 103 (1988).
[50] L. E. Fried and G. S. Ezra, J. Phys. Chem. **92**, 3144 (1988).
[51] T. Komatsuzaki and R. S. Berry, Proc. Nat. Acad. Sci. USA **98**, 7666 (2001).
[52] G. D. Birkoff, *Dynamical Systems* (American Mathematical Society, New York, 1927).
[53] F. Gustavson, Astron. J. **21**, 670 (1966).
[54] W. H. Press, S. A. Teukolsky, W. T. Vetterling, and B. P. Flannery, *Numerical Recipes*, 2nd ed. (Cambridge University Press, New York, 1992).
[55] B. J. Gertner, K. R. Wilson, and J. T. Hynes, J. Chem. Phys. **90**, 3537 (1989).
[56] We chose the minimum bound of τ to be taken into account to be ($\cong 0.5$), as inferred from Fig. 4: while all the approximate invariants of action associated with nonreactive dofs are ruined for $\tau \gtrsim 0.5$, the approximate invariant of action stands out along $\bar{q}_1^{\mathrm{2nd}}(\mathbf{p},\mathbf{q})$ even after $\tau \cong 0.5$.
[57] S. A. Rice and M. Zhao, *Optical Control of Molecular Dynamics* (Wiley, New York, 2000).
[58] R. Hernandez and W. H. Miller, Chem. Phys. Lett. **214**, 129 (1993).
[59] D. Sugny and M. Joyeux, J. Chem. Phys. **112**, 31 (2000).
[60] C. C. Martens, M. J. Davis, and G. S. Ezra, Chem. Phys. Lett. **142**, 519 (1987).
[61] J. Laskar, Icarus **88**, 266 (1990).
[62] J. C. Losada, J. M. Estebaranz, R. N. Benito, and F. Borondo, J. Chem. Phys. **108**, 63 (1998).